IONIZATION OF ALKALI METAL ATOMS BY SLOW ELECTRONS

I. P. ZAPESOCHNYĬ and I. S. ALEKSAKHIN

Uzhgorod State University

Submitted January 14, 1968

Zh. Eksp. Teor. Fiz. 55, 76–85 (July, 1968)

An improved technique for studying ionization in crossed atomic and monoenergetic electron beams is described. The ionization cross sections are measured for all alkali metals at electron energies from threshold to 30 eV. The linear increase of the cross sections that is predicted by Geltman's theory at the ionization threshold is observed, and the linear interval is determined for each atom. The complex structure observed in the cesium, rubidium, and potassium ionization curves can be accounted for consistently and uniquely by p-electron excitation of the alkali atom followed by its ionization with ejection of the p electron.

INTRODUCTION

THE ionization of alkali metal atoms by electron impact has been investigated frequently.[1-7] Tate and Smith[1] were the first to measure the ionization functions of sodium, potassium, rubidium and cesium, using volumes of the metal vapors. Using a variant of that technique, one of the present authors measured the ionization cross sections of potassium and cesium.[4] The crossed beam technique was used in[5,6] to measure the cross sections for ionization of alkali atoms by electrons from 50 to 500 eV, and to obtain the cross sections in the region (10–30 eV) of maximum efficiency.

The behavior of the ionization function at threshold for different alkali atoms has been studied in[2] and in[7] by the volume of gas technique, and in[3] by means of crossed beams. However, these publications contain no discussion of the threshold behavior. Theoretical studies had previously indicated two different dependences of the ionization cross section on the excess energy possessed by the electrons above threshold. Geltman[8] predicted a linear law, while Wannier predicted a power law with the exponent 1.127.[9]

It therefore became necessary to perform new experiments in which alkali atom ionization by low-energy electrons would be investigated systematically and thoroughly. Our work was undertaken to develop a sufficiently reliable means of determining the absolute ionization cross sections and to perform careful ionization measurements for all alkali atoms near threshold, including the region of maximum efficiency.

APPARATUS AND EXPERIMENTAL TECHNIQUE

Our experiments were based on the crossed beam technique, which was first used by Funk,[10] and later by other workers, to investigate the ionization of atoms. We made further improvements by using electron beams having a small energy spread and also a new means of measuring the neutral particle density in the atomic beam.

The main units of the apparatus are: 1) an atom furnace, 2) a detector of neutral atom density, 3) a 127-degree electrostatic electron selector, and 4) an ion registration unit. The first three of these units

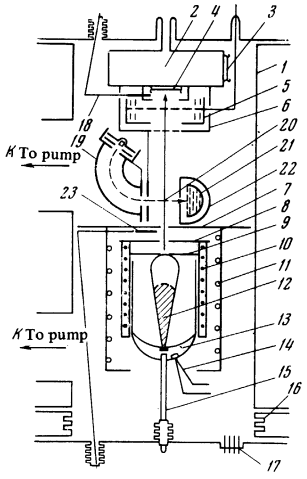

FIG. 1. Apparatus: 1–housing of chamber, 2–container of liquid nitrogen, 3–quartz reference crystal, 4–quartz measuring crystal, 5–ion collector, 6–quard cylinder, 7–cold slit, 8, 9–hot slits, 10–heating coils, 11–cooling pipe, 12–ampoule containing test material, 13–container, 14–thermocouple, 15–rod with bellows, 16–adjusting bellows, 17–vacuum electric leads, 18–shutter of quartz measuring crystal, 19–electron monochromator, 20–beam intersection region, 21–electron receiver, 22–guard cylinder, 23–atom furnace damper.

were placed inside the vacuum chamber (Fig. 1), which was made of stainless steel with metallic seals. Following the requisite heating of the chamber the residual pressure during measurements was $(0.5-1) \times 10^{-7}$ Torr. The sources of neutral atoms were effusion chambers,[11] which are of simple construction and furnish a very stable atom beam for a protracted period of time. Metal atoms evaporated from the chamber; a beam was formed with the aid of two hot slits and one cold slit, having the respective dimensions 0.2×1 mm and

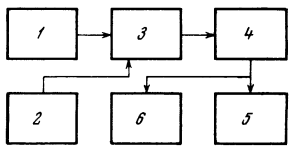

FIG. 2. Schematic for measurement of neutral atom intensity in the beam.

5 × 6 mm. Stainless steel was used for both the effusion chamber and the slits, and the atom beam spread was at most six degrees.

The techniques described in the literature for measuring atom intensities in beams[11] suffer from several deficiencies, including low accuracy and limited applicability. We therefore used an electronic technique, determining the mass of atoms condensed on the surface of a piezoelectric quartz crystal (cooled by liquid nitrogen) from the change of natural vibrational frequency. This change is directly proportional to the mass M_k of condensed material:[12,13]

$$\Delta f = (k_f S)^{-1} M_k, \qquad (1)$$

where S is the area of the condensate on the crystal and k_f is a constant that depends on the crystal cut and frequency. We used AT-cut quartz having the natural frequency $f_0 = 4.79 \times 10^6$ Hz.

The circuit used to determine the frequency change (Fig. 2) consists of a quartz measuring oscillator 1, a reference oscillator 2, a frequency mixer 3, a difference frequency amplifier 4, a frequency meter 5, and an oscillograph 6 for monitoring the shape of the low-frequency signal. The measuring and reference crystals were attached to a liquid nitrogen trap (Fig. 1). We obtained ± 5 Hz frequency stability during a period of 5 minutes (the usual experimental period). The constant k_f was calculated[13] and was also determined experimentally with a torsion balance; agreement, with 3% error, was obtained for the value 1.9×10^{-8} g-Hz^{-1}-cm^{-2}.

The density of atoms in the collision region was determined from the equation

$$n = M_k / t\bar{v}lbm, \qquad (2)$$

where l and b are the dimensions of the atom beam (2.6×6 mm) where it is crossed by the electron beam, t is the time during which atoms condensed on the piezocrystal, $\bar{v}$ is the mean velocity of beam atoms, and m is the atomic mass.[1)] The atom concentration in this region was varied, by changing the source temperature, between the limits 1×10^{11} and 6×10^{11} atoms/cm^3.

A monoenergetic electron beam was formed by apparatus that included a 127-degree electrostatic selector.[14] A flat beam with a velocity spread of only 0.5 eV for 90% of the electrons was obtained from a conventional electron gun with an indirectly heated oxide ribbon cathode. All parts of the electron monochromator, made of stainless steel, were specially treated, and were then assembled and adjusted under a microscope. This type of monochromator provided electron beams with an 0.1-eV energy spread for 90% of all electrons at intensities from 0.05 to 0.1 μA in the energy range 1–30 eV.

The electron monochromator was rigidly attached at the cold slit, and the distance from the first hot slit of the atom furnace to the region of beam crossing was at most 3 cm. The electron beam crossed a broad segment of the atom beam, so that all beam electrons penetrated the atom beam, thus excluding errors arising from beam defocusing at low energies.

[1)] It is assumed in (2) that the condensation coefficient of alkali metals on a quartz surface is unity at liquid nitrogen temperature after the surface has been covered with a layer of the same metal.

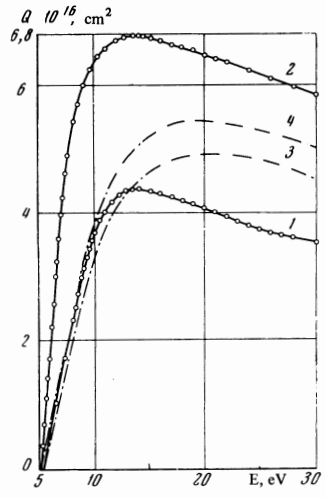

FIG. 3. Ionization cross sections of lithium and sodium. 1 and 2—our results; 3 and 4—calculations in Gryzinski's approximation.

The potential applied to the ion collector was 1 V below the cathode potential of the electronic system. The ion current was therefore saturated, and scattered electrons did not impinge on the ion collector. To prevent the field due to these potentials from seriously affecting the electron energy distribution, a thick tungsten grid allowing 90% transmission was positioned at the entrance of the guard cylinder. Current from the ion collector was fed to a U1-2 electrometric amplifier.

The formula used to calculate atomic ionization cross sections at fixed electron energies is

$$Q = c \frac{i_{\text{ion}}}{i_e} \frac{l\sqrt{mT}}{M_k} t, \qquad (3)$$

where M_k is obtained from (1), i_{ion} is the ion current, i_e is the electron current, T is the absolute temperature of the metal vapor in the source, and $c = 2.2 \times 10^{-8}$ cm-sec^{-1}-g$^{1/2}$-deg$^{-1/2}$ is the constant of the method.

Relative ionization curves were obtained with a spread of at most 3–5%. The absolute values of the ion current (10^{-12}–10^{-13} A) were measured, as a rule, at the ionization maximum, when the contribution from residual gas ionization was negligible [< 1 for p = (0.5–1)

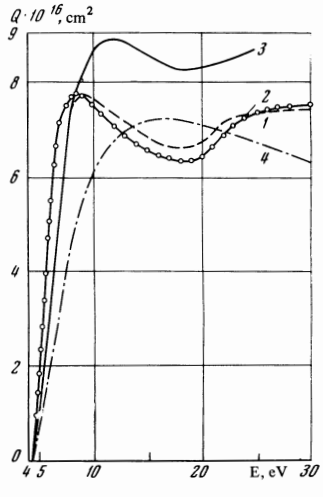

FIG. 4. Ionization cross section of potassium. 1—our results; 2—obtained by Tate and Smith [1]; 3—obtained by Korchevoĭ and Przhonskiĭ [7]; 4—calculated using Grysinski's formula.

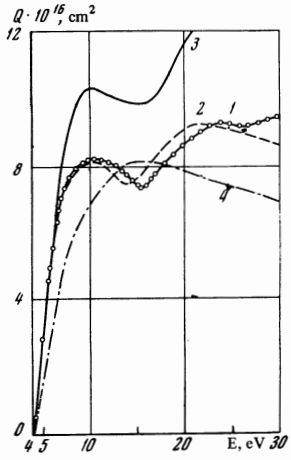

FIG. 5. Ionization cross section of rubidium. 1—our results; 2—obtained by Tate and Smith; 3—obtained by Korchevoĭ and Przhonskiĭ; 4—calculated using Grysinski's formula.

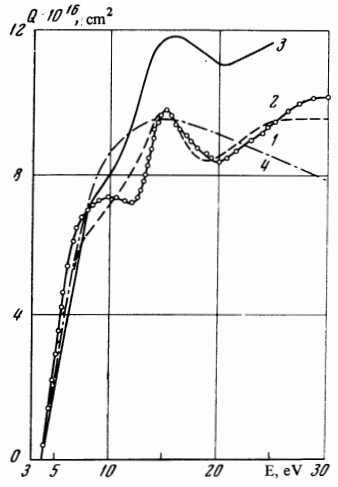

FIG. 6. Cross section of cesium. 1—our results; 2—obtained by Tate and Smith; 3—obtained by Korchevoi and Przhonskii; 4—calculated using Gryzinski's formula.

$\times 10^{-7}$ Torr].[2)] The relative error of the absolute cross sections is ±15%, and the rms error is +12%.

Control measurements showed that our technique for investigating atomic ionization cross sections is characterized by high sensitivity (10^{14}—10^{15} atoms/sec), universality, satisfactory accuracy, and very good energy resolution of the ionization curve structure.

RESULTS AND DISCUSSION

We investigated the ionization of five alkali atoms at energies from threshold to 30 eV.[3)] The behavior of the ionization curves was investigated especially thoroughly at threshold and at the ionization maxima. Most of the relative and absolute measurements were visual readings of a precision pointer-type instrument; other measurements (of the ionization curves) were obtained with a recording electronic potentiometer. In the last instance the electron energy was given by a special potentiometer which was rotated by a synchronous motor.

The absolute cross section measurements were repeated nine or more times while varying the electron and atom densities and with different geometries for the beam crossing region.

Our principal results are presented in Figs. 3—8 and in the table. The horizontal axis of the drawings represents the electron energy in electron volts with 0.1—0.2 eV uncertainty. The vertical axis in Figs. 3—6 represents absolute ionization cross sections in cm^2, and in Figs. 7 and 8 represents relative cross sections in arbitrary units.

1. Complex structure of ionization functions and its origin

We shall first consider the ionization functions of the atoms. The curves for different atoms are characterized by an absence of similarity in their behavior at low energies. The ionization functions of lithium and sodium exhibit the simplest form, with one broad peak; the curves for potassium and rubidium have two maxima,

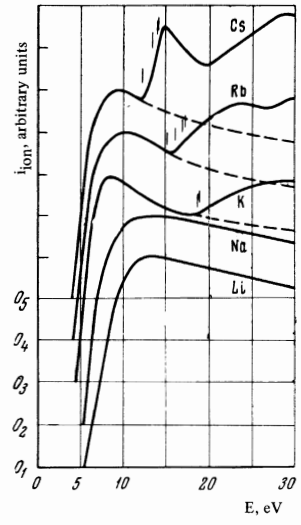

FIG. 7. Ionization functions of alkali metal atoms. The vertical bars designate the energies of the lowest levels in the case of p-electron excitation.

and that for cesium has three.[4)] We observe a gradual shift toward lower energies of the first peaks as the atomic number increases. A similar tendency of the second maxima for K, Rb, and Cs is also observed.

A comparison of our curves with those of Tate and Smith (whose curves are normalized according to our absolute measurements in Figs. 3—6) shows that the latter obtained essentially correct ionization functions of K and Rb. Like all other authors, they fail to show the first peak for Cs. For the same elements two maxima were obtained, although less distinctly, in[7].

It is obvious that the clear first peak (at 9.5 eV) of the ionization function of cesium, which was first discovered by us, along with the improved sharpness and accuracy of all other ionization maxima of alkali atoms result directly from the more advanced technology used in our experimental work.

The ionization functions of all the atoms are collected in Fig. 7 for convenience in connection with further discussion. We believe that the complete and unequivocal explanation of the complexity of these curves can be derived from the fact that when electrons collide with

[2)] It was therefore unnecessary to further complicate the procedure by modulating the atom beam.[5]

[3)] Our results pertain to single ionization, since the double-ionization threshold of practically all alkali metal atoms exceeds 30 eV. However, for the one exception, rubidium, $E^{++} = 27$ eV.

[4)] We mentioned a peak at E ~ 10 eV in [4].

Element	Ionization potential E_i eV	Maxima E, eV	Linear interval Δe, eV	Slope of straight segment, 10^{-16} cm^{-2}/V	Q_{max}, 10^{-16} cm^2		
					Our result	[5]	[6]
Li	5.39	~13.0	3.4	0.9	4.2	—	4.9
Na	5.14	~14.0	1.5	2.4	6.8	8.6	7.6
K	4.34	8.5; ~27.0	1.2	3.6	7.9	9.6	8.2
Rb	4.18	10.5; 24.0	1.1	3.2	—	9.6	8.2
Cs	3.89	9.5; 15.0; ~29.0	1.0	2.6	10.2	11.2	9.4

alkali metal atoms the kinetic energy of the electrons is transferred both to s electrons and to inner p electrons of the alkali atoms.

Let us therefore consider the most complex ionization, which is observed in the case of cesium. The first peak (see the table) can here reasonably be attributed to ordinary s-electron ionization:

$$A + e \rightarrow A_s^+ + 2e, \tag{4}$$

where A and A_S^+ are the neutral atom and the ordinary ion. The second and third maxima arise through p-electron excitation and ionization:

$$A + e \rightarrow A_p^* + e \rightarrow A_s^+ + 2e, \tag{5}$$

$$A + e \rightarrow A_p^+ + 2e, \tag{6}$$

where A_p^* and A_p^+ are the excited atom and the ion (minus a p-electron).

The foregoing account is confirmed, first of all, by the level scheme of Cs in the case of p-electron excitation.[15] The group of the lowest excited levels is here 12.3, 13.5, 14.1, and 14.2 eV. Autoionization (5) then converts these excited atoms into states of ordinary ions, and at about 12–13 eV the ionization curve begins to rise steeply to a maximum at 15 eV. On the other hand, the four ionization limits of Cs for the detachment of a p electron are 17.2, 17.5, 18.8, and 19.1 eV. This type of ionization obviously causes the third maximum of Cs ionization, beginning at 18–20 eV.

Secondly, the maximum at 15 eV is clearly revealed in all the excitation functions of cesium lines from the ^2S, ^2P, and ^2D levels, whose relative roles increase with the higher principal quantum number of the level.[16] This maximum is also uniquely associated with the aforementioned group of excited Cs levels (p-electron transitions). Some of the excited states of A_p^* undergo cascade transitions to ordinary excited states of cesium.

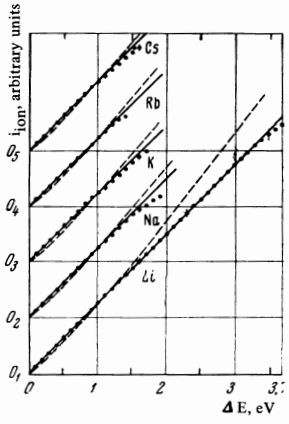

FIG. 8. Ionization curves of alkali atoms near threshold. ●–experimental data; sold lines–calculated using Geltman's theory; dashed lines–calculated using Wannier's theory. The average spread of the points is denoted by the vertical bars.

For rubidium the excitation energy involving the analogous group of p levels is considerably higher (15.2, 16.2, 17.0, and 17.3 eV); this leads to a corresponding shift of the second ionization curve maximum. The location of the second maximum (and its beginning) is shifted still more in the case of potassium, whose excited p states encompass the interval 18.7–20 eV.

Since according to Moore[15] the limits of the excited p levels of lithium and sodium are 34 and 54 eV, respectively, we can understand why the ionization functions of these elements exhibit no nonmonotonic behavior (in our energy range).

From the foregoing we conclude that ordinary ionization (the detachment of an s electron) is observed in its pure (simple) form only in the cases of lithium and sodium, but that in the heavier alkali atoms it is masked by additional ion-formation processes, for which p electrons are responsible.

We note here that the hypothesis of p-electron participation in the ionization of potassium and rubidium was previously presented by Kaneko[3] and by Brink,[5] who were unable, however, to extend the hypothesis to cesium. (It is now clear that their failure to do this resulted from very crude measurements of the cesium ionization curve in earlier work.) Therefore the character of cesium ionization that we have observed furnishes a clue to a consistent and unequivocal explanation of the ionization-curve behavior for all the alkali atoms near threshold.

The dashed lines in Fig. 7 distinguish simple ionization from the other processes for potassium, rubidium, and cesium.[5)] We observe, on the one hand, that the cross sections for ordinary ionization of all five atoms have very similar energy dependence. On the other hand, for certain incident electron energies the p electrons make very large contributions to the ionization of Cs, Rb, and K.

2. Ionization cross sections at low energies

The absolute ionization cross sections for the greatest maxima are given in the table, while Figs. 3–6 show the cross sections for the entire energy interval.[6)] Our results are in good general agreement with those in[6] and in[7], especially with the first of these. The differences between the results obtained in the three investigations lie practically within the limits of experimental error, although in[7] the absolute cross sections are a little too large and the positions of the maxima were determined with considerably less accuracy.

The fact that three investigations using very different techniques are in agreement, within experimental error limits, indicates that we now have reliable ionization cross sections of alkali atoms both at low energies (our results), and in the region 30–500 eV.[6]

Figures 3–6 also show that the experimental results are in satisfactory general agreement in the regions of the maxima with the cross sections that we calculated

[5)] Of course, these curves have been plotted with a certain degree of arbitrariness.

[6)] We did not measure the absolute cross section for rubidium ionization; the obtained ionization function was normalized in accordance with the results given in [6] for the principal maximum.

using Gryzinski's method.[17] To be sure, the behavior of these ionization curves is far from agreeing with experiment in regard to the complex structure of the ionization functions or the positions of the maxima, which are shifted toward higher energies by a factor of about 2.

It must be emphasized, however, that the calculated curves exhibit considerably closer resemblance to the ionization curves associated with the detachment of a single s electron. This is in accord with our purpose in calculating the cross sections for alkali atoms.

3. The behavior of the ionization curves near threshold

Figure 8 shows the ionization curves at threshold for all the alkali metals. The difference ΔE between the incoming electron energy (E) and the ionization potential (E_i) of a given atom is plotted horizontally. The relative errors of these particularly careful experiments do not exceed 3%.

The curves are characterized by almost linear intervals, from a length of 1.0 eV for cesium to 3.4 eV for lithium. We have already mentioned in our Introduction that one theory predicts these initial segments of the ionization curves but that it does not furnish information about the lengths of the intervals.

As a basis for an objective discussion regarding the correctness of either particular theory, we have in Fig. 8 plotted both groups of calculated curves: those representing Wannier's theory $\varphi(\Delta E) \sim \Delta E^{1.127}$ and Geltman's linear law. The curves were normalized at the origin $\Delta E = 0$ and at $\Delta E = 1$, where the two theories yield identical results.

For cesium and rubidium the smallness of the intervals makes it difficult to choose between the theories; in the region of excess energy from 0 to 1 eV the difference between the calculated curves is practically no larger than the error of relative measurements for the ionization curves. For sodium and potassium we already observe a tendency to favor the linear law of initial ionization.

Only in the case of lithium with its large linear interval[18] can we see clearly that the experimental points fit a straight line. We can therefore affirm unequivocally that (at least for lithium) Wannier's prediction is unconfirmed and that Geltman's linear theory is correct

Ionization of atoms by electron impact has thus been found to be considerably more complex than had been anticipated. A comprehensive and careful investigation could therefore obtain valuable and extensive knowledge regarding the characteristics of inelastic electron-atom collisions.

The authors are indebted to I. I. Garga and E. I. Meteleshko for technical assistance.

[1] J. T. Tate and P. T. Smith, Phys. Rev. **46**, 773 (1934).
[2] V. H. Dibeler and R. M. Reese, J. Chem. Phys. **31**, 282 (1959).
[3] Y. Kaneko, J. Phys. Soc. Japan **16**, 2288 (1961).
[4] I. S. Aleksakhin, A. I. Imre, and I. F. Kovalenko, Tezisy dokladov i soobshcheniĭ UzhGU, ser. fiz.-matem. nauk, 1964, p. 98.
[5] G. O. Brink, Phys. Rev. **127**, 1204 (1962) and **134**, A345 (1964).
[6] R. H. McFarland and J. D. Kinney, Phys. Rev. **137**, A1058 (1965).
[7] Yu. P. Korchevoĭ and A. M. Przhonskiĭ, Zh. Eksp. Teor. Fiz. **51**, 1617 (1966) [Sov. Phys.-JETP **24**, 1089 (1967)].
[8] S. Geltman, Phys. Rev. **102**, 171 (1956).
[9] G. H. Wannier, Phys. Rev. **90**, 817 (1953).
[10] H. Funk, Ann. Physik **4**, 149 (1930).
[11] N. F. Ramsey, Molecular Beams, Clarendon Press, Oxford, 1956 (Russ. transl., IIL, 1960).
[12] G. Sauerbrey, Z. Physik **155**, 206 (1959).
[13] A. I. Akishin and V. S. Zazulin, Pribory i tekh. éksper. No. 1, 152 (1963).
[14] I. P. Zapesochnyĭ and O. B. Shpenik, Zh. Eksp. Teor. Fiz. **50**, 890 (1966) [Sov. Phys.-JETP **23**, 592 (1966)].
[15] C. E. Moore, Natl. Bur. Std. (U.S.) Circ. No. 467, vol. I, 1949; vol. II, 1952; vol. III, 1958.
[16] I. P. Zapesochnyĭ and L. L. Shimon, Opt. i Spektroskopiya **20**, 753 (1966) [Opt. Spectry **20**, 421 (1966)].
[17] M. Gryzinski, Phys. Rev. **115**, 374 (1959).
[18] I. S. Aleksakhin, I. P. Zapesochny and O. B. Shpenik, Fifth. Intern. Conf. Phys. Electr.-At. Collisions (Abstracts of Papers), Leningrad, 1967, p. 499.

Translated by I. Emin
9